Pergamon

Int. J. Heat Mass Transfer. Vol. 38, No. 14, pp. 2549–2556, 1995

0017-9310/95 $9.50+0.00

0017-9310(95)00011-9

An analytical method for determining thermal conductivity from dynamic experiments

ROSEMARY A. MACDONALD

Thermophysics Division, National Institute of Standards and Technology, Gaithersburgh, MD 20899, U.S.A.

(*Received* 4 *April* 1994 *and in final form* 13 *December* 1994)

Abstract—The temperature profile along a cylindrical rod or tube as it cools has been obtained by numerical solution of the second-order time-dependent partial differential equation for heat conduction. The surface temperature is calculated for given temperature dependent values of the heat capacity, hemispherical total emissivity, thermal expansion and thermal conductivity and, by adjusting the thermal conductivity, is fitted to experimental temperature profiles obtained from preliminary measurements on a cooling cylindrical tungsten rod. The surface temperature of the rod is quite sensitive to the thermal conductivity but the accuracy of the predicted thermal conductivity cannot be assessed without further experimentation.

1. INTRODUCTION

An analytical method is described for determining the thermal conductivity of a cylindrical metal rod, or tube, at high temperatures from subsecond measurements of its time dependent surface temperature profile as the cylinder is either heated or cooled. The use of high speed measurement techniques reduces problems of sample degradation that arise in steady state methods at these temperatures. The method involves the matching of the experimental profiles to those calculated from the heat flow equation with a specific form for the thermal conductivity $\kappa(T)$. If this is to be a viable method, (a) the surface temperature must be sensitive to this property and (b) it must be demonstrated that parameters representing the thermal conductivity in the calculation can be determined accurately by comparing the calculated surface temperature with experiment.

In order to carry out this investigation, preliminary results on the temperature profile obtained by a high speed pyrometer [1] that sweeps the length of a tungsten rod in millisecond intervals, as the rod cools, have been made available [2].

2. THEORY

The problem is to find the temperature profile along a cylinder of radius a, length L_0, at time $t > 0$ during Joule heating or subsequent cooling when heat loss occurs by conduction to the end clamps and by thermal radiation into a vacuum (hence no convective loss), the container being maintained at an ambient temperature $T = T_0$. The cylinder has total hemispherical emissivity ε, thermal conductivity κ, thermal expansion α and heat capacity at constant pressure C, and an initial temperature distribution $T(r, z, t_0)$ such that the surface temperature is $T^{\exp}(z, t_0)$ at the time origin $t = t_0$.

The heat flow equation for this system is as follows [3]:

$$\delta C\,\partial T(r,z,t)/\partial t = (1/r)\,\partial[r\kappa(r,z)\,\partial T(r,z,t)/\partial r]/\partial r + \partial[\kappa(r,z)\,\partial T(r,z,t)/\partial z]/\partial z + \rho(r,z)j^2(r,z) - \mu(r,z)[j(r,z,t)\cdot\nabla T(r,z,t)] \quad (1)$$

where C and δ, the density, are implicit functions of r and z through their dependence on temperature, $\rho(r, z)$ is the electrical resistivity, $j(r, z, t)$ is the electrical current density, and $\mu(r, z)$ is the Thomson coefficient. When the cylinder is cooling after the current has been cut off, this equation simplifies to

$$\delta C\,\partial T(r,z,t)/\partial t = (1/r)\,\partial[r\kappa(r,z)\,\partial T(r,z,t)/\partial r]/\partial r + \partial[\kappa(r,z)\,\partial T(r,z,t)/\partial z]/\partial z. \quad (2)$$

These equations are to be solved under the appropriate initial and boundary conditions.

On heating, the initial condition is, ideally, $T(r, z, t_0) = T_0$ for all r and z. On cooling, $T(r, z, t_0)$ is set to the experimentally observed surface temperature profile at the chosen time origin t_0. In practice, this is also done on heating because the temperature at the ends of the cylinder cannot be maintained at T_0 and their actual temperature is not measured.

The boundary conditions are quite complex for two reasons: (1) the pyrometer is not accurate at temperatures below about 1500 K so a temperature is not recorded until some distance from the ends of the cylinder and (2) for a tube, there is a complicated pattern of radiation gain and loss at the inside surface which must be taken into account. In the longitudinal direction, a length of cylinder is chosen so that it is at a high enough temperature to be measured accurately

NOMENCLATURE

- a outer radius of rod or tube [m]
- b inner radius of tube [m]
- C heat capacity at constant pressure [J kg^{-1} K^{-1}]
- F factor in radial boundary condition for tube
- G_{ij} geometric factor in radial boundary condition for tube
- G'_{ij} geometric factor in radial boundary condition at ends of tube
- j electrical current density [A m^{-2}]
- $L(t)$ length of rod between two designated points at time t [m]
- L_0 length of rod at ambient temperature [m]
- N number of segments in section of rod selected for study
- p pixel size [m]
- r radial position in rod or tube [m]
- t time [s]
- t_i time of ith temperature profile [s]
- $T(r, z, t)$ temperature at position (r, z) in rod at time t [K]
- $T^{\exp}(z, t)$ surface temperature at position z on rod at time t [K]
- T_0 ambient temperature [K]
- $y(T/T_0)$ general polynomial representation of temperature dependent property (dimensions of property)
- y_i coefficients of y (dimensions of property)
- z axial position in rod [m]
- z_i axial position of ith segment of selected section of rod [m].

Greek symbols

- α linear thermal expansion
- δ density of specimen [kg m^{-3}]
- δT_i radial increment in temperature for initial and boundary conditions [K]
- δz length of segment of rod at initial condition [m]
- $\Delta(z, t)$ fractional difference between calculated and experimental surface temperature at position z, time t
- $\Delta T(z, t)$ difference between calculated and experimental surface temperature at position z, time t [K]
- ε hemispherical total emmittance
- γ_{ij} coefficients in time dependent boundary conditions at ends of selected section of rod
- κ thermal conductivity [W m^{-1} K^{-1}]
- κ_i coefficients in polynomial representation of thermal conductivity [W m^{-1} K^{-1}]
- μ Thomson coefficient [Ω A K^{-1}]
- ρ electrical resistivity [Ω m]
- σ Stefan–Boltzmann constant [W m^{-2} K^{-4}].

Subscripts and superscripts

- exp experimental values
- i, j running indices
- o original value.

over a selected time interval. Then, for the chosen length containing N segments, the boundary conditions are represented by the following quadratic equations in time:

$$T(a, z_1, t) = T^{\exp}(z_1, t_0) + \gamma_{11}(t - t_0) + \gamma_{12}(t - t_0)^2 \quad (3)$$

$$T(a, z_N, t) = T^{\exp}(z_N, t_0) + \gamma_{21}(t - t_0) + \gamma_{22}(t - t_0)^2 \quad (4)$$

where the γ_{ij} are matched to the experimental profiles at the chosen end points. Lacking experimental data for the interior of the cylinder, the temperature gradient is assumed to have a constant value over the cross section at these two boundaries, i.e.

$$T(r, z_1, t) = T(a, z_1, t) + \delta T_1 (a - r)/a \quad (5)$$

and

$$T(r, z_N, t) = T(a, z_N, t) + \delta T_N (a - r)/a. \quad (6)$$

To start the calculation, δT_i was taken to be zero but, subsequently, it was assumed to have a value consistent with the variation of temperature with r that was actually observed in the computed results close to, but away, from the end points. Values of the order of 10 K are typical.

In the radial direction, for both the rod and the tube, the boundary condition at $r = a$ is

$$-\kappa(r, z)\, \partial T(r, z, t)/\partial r|_{r=a} = \varepsilon(a, z)\sigma[T^4(a, z, t) - T_0^4] \quad (7)$$

where σ is the Stefan–Boltzmann constant. For the rod, the symmetry condition at $r = 0$ is

$$\partial T(r, z, t)/\partial r|_{r=0} = 0 \quad (8)$$

and for the tube with inner radius b, the boundary condition at $r = b$ is

$$\kappa(r, z)\, \partial T(r, z, t)/\partial r|_{r=b} = \varepsilon(b, z)\sigma\left[T^4(b, z, t) - \frac{F(b, z)}{4b} T_0^4\right] \quad (9)$$

where

$$F(b,z_i)=\sum_{j=1}^{j=N}\varepsilon(b,z_{ij})T^4(b,z_{ij},t)\delta z_j G_{ij}$$

$$+\varepsilon(b,z_{i1})T^4(b,z_{i1},t)G'_{i1}+\varepsilon(b,z_{iN})T^4(b,z_{iN},t)G'_{iN}. \quad (10)$$

$z_{ij}=z_i-z_j$, δz_i is the width of the element at $z=z_i$ and G_{ij} and G'_{ij} are geometric factors which depend on the separation between elements z_i and z_j according to the relations

$$G_{ij}=\frac{[(z_{ij}^2+4b^2)^{3/2}-z_{ij}^3-6z_{ij}b]}{(z_{ij}^2+4b^2)^{3/2}} \quad (11)$$

$$G'_{ij}=2\left[\frac{z_{ij}^2+2b^2}{(z_{ij}^2+4b^2)^{1/2}}-z_{ij}\right]. \quad (12)$$

The factor G'_{ij} accounts for the end faces of the tube. Noting that the difference between the rod and the tube enters only in these radial boundary conditions, in the rest of the paper, unless specified otherwise, the discussion will refer to the rod.

3. CALCULATIONS

The temperature profile $T(r,z,t)$ is calculated directly by use of the software package for solution of non-linear partial differential equations, PDETWO [4]. Thermal expansion is taken into account in the z-direction only: the section of the rod under consideration, having a length $L(t_0)$ measured in meters, is divided into N equal segments, $\delta z=L(t_0)/N$, each of which is adjusted in size at later times according to its surface temperature $T(a,z,t)$ and the linear thermal expansion coefficient $\alpha(T)$. Although this is a small effect, it does result in a length contraction of a few pixels in the course of the experiment. Lengths in the radial direction are scaled in units of the outer radius a. Thermal expansion is ignored in this direction, partly because of the added complications it would involve and partly because the calculations show that temperature differences in the radial direction are so small. The temperature is scaled in units of T_0, the ambient temperature.

3.1. *Temperature dependence*

The temperature-dependent properties which are pertinent to the cooling situation, C, κ, ε and α, are represented in the general form

$$y(T/T_0)=y_0+y_1(T/T_0)+y_2(T/T_0)^2+\ldots \quad (13)$$

For C, ε and α, the coefficients y_0, y_1, y_2, etc. have been obtained by fitting to experimental data for tungsten [5, 6]. The thermal conductivity coefficients κ_0, κ_1 and κ_2, are to be determined by comparing the computed temperature profiles with those obtained experimentally.

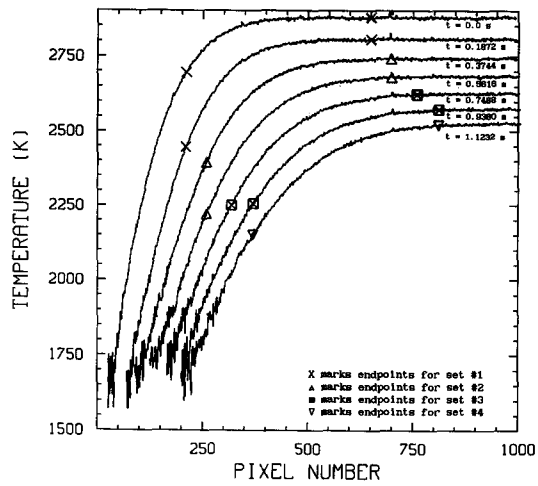

Fig. 1. Experimental surface temperature profiles for cooling rod. True temperature [K] vs pixel number at intervals of 0.1872 s from $t=0$ to $t=1.1232$ s. The endpoints of the sections actually used for comparison with the calculations are indicated by symbols as indicated.

3.2. *Preparation of experimental data for use in analysis*

The experimental data consists of surface temperatures as a function of distance along the rod from near the clamped end to the center at regular time intervals (0.0936 s) as it cools. The other end of the rod is free to move as the rod contracts. Figure 1 shows an example of a preliminary data set [2]. Here, true temperature profiles are plotted as a function of the pixel number of the pyrometer at intervals of 0.1872 s (the alternate profiles have been omitted for the sake of clarity). The pixel size is 2.8325×10^{-5} m.

In order to obtain the initial condition and the boundary conditions at the ends of the chosen section for use in the calculations, and for ease of comparison between theory and experiment at later times, it is necessary to smooth the data. Smoothed values of the surface temperature $T^{\exp}(z,t)$ are obtained from a program SMOOTH [7] which uses cubic splines to fit the experimental data within prescribed tolerances. The smoothed curve taken as the initial condition for cooling and its corresponding experimental data are shown in Fig. 2 together with a plot of the residuals of this fit. Similar fits to the experimental data are obtained at successive intervals of 0.0936 s, and it is these smoothed profiles which will be referred to as $T^{\exp}(z,t)$ in all that follows.

Comparison between the calculated and experimental profiles focuses on the region of the rod most sensitive to the thermal conductivity where the longitudinal temperature gradient is greatest. Since the lower endpoint, z_1, is to be held at a constant pixel number, at some later time the temperature at this point will fall into the region where $T^{\exp}(z_1,t)$ cannot meet the required tolerance on the fit. As can be seen from Fig. 1, where X marks the endpoints selected for the first set of profiles, this would be the case for the profile at $t=0.5616$ s (profile No. 6). Therefore, for

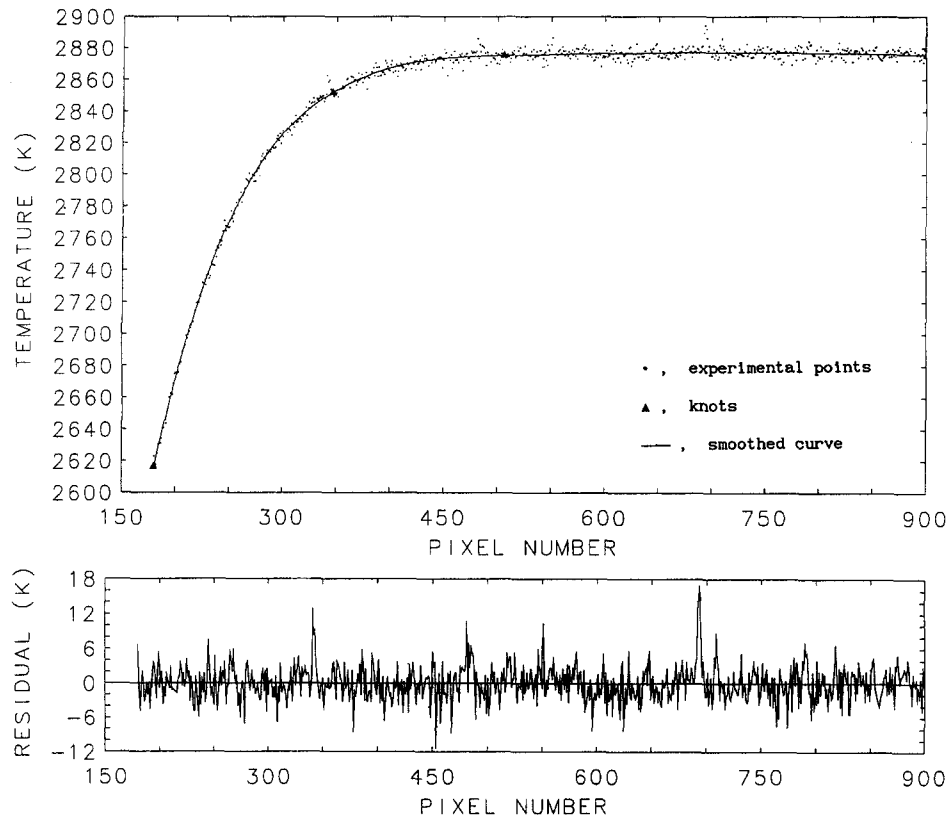

Fig. 2. Smoothing of the experimental data. Upper curve shows smoothed curve and experimental points for the temperature profile chosen as time origin for set No. 1. Spline degree = 3, number of knots = 10. Lower curve shows residuals of the fit.

this and subsequent profiles, z_1 must be moved to a higher pixel number. For the data set under examination here, it is convenient to break the time range into four overlapping sets of five profiles, the fourth profile of one set being the initial condition for the next set. The upper end point z_N is not critical so long as it is in the region where the temperature is essentially constant. To clarify this discussion, the end points for each set are indicated in Fig. 1. Once the endpoints and number of profiles to be included in a set have been decided upon, the time dependence of the endpoint temperatures is obtained by fitting them to equations (3) and (4). This can be done to better than 5 K—well within the scatter of the data.

3.3. *Procedure*

The comparison between calculation and experiment is monitored by the fractional difference,

$$\Delta(z,t) = [T(a,z,t) - T^{\exp}(z,t)]/T^{\exp}(a,z,t) \quad (14)$$

plotted against temperature, $T(a,z,t)$: monitoring the fractional difference makes it easier to compare the fit at different times and plotting against temperature rather than distance along the rod makes it easier to monitor the situation as κ_0, κ_1 and κ_2 are varied since κ is a function of T.

First, with $\kappa_1 = \kappa_2 = 0$, $\Delta(z,t)$ is calculated for a range of values of κ_0 such that $\Delta(z,t)$ changes from being predominantly positive to predominantly negative as κ_0 changes from κ_0^i to κ_0^{i+1}: the perfect fit would be $\Delta(z,t) = 0$ for all z and t. This narrows the range of values that κ can take in the temperature region under consideration. Next, κ_0 and κ_1 are found such that $\kappa(T_1) = \kappa_0^i$ at one temperature T_1 where $\Delta(z,t)$ is close to zero and $\kappa(T_2) = \kappa_0^{i+1}$ at another such temperature T_2. Small adjustments in κ_0 and κ_1 are made to improve the fit over the whole profile at all times in the set. Finally, if addition of a quadratic term in κ is warranted, using $\Delta(z,t)$ for the best pair of values (κ_0, κ_1) as a guide, adjustments made to $\kappa(T)$ at three temperatures are used to determine κ_0, κ_1 and κ_2. Further small adjustments of these parameters may be necessary to arrive at a "best" fit.

4. RESULTS

The preliminary measurements that have been made available for testing this method of analysis were made on a cylindrical tungsten rod as it cooled [2]. The specifications of the rod are given in Table 1, together with the coefficients y_0, y_1, to y_n that represent the data for C, α and ε. All values of κ_0, κ_1 and κ_2 are in W m^{-1} K^{-1}. The length of rod quoted is the half length over which measurements were actually made

Table 1. Specifications for tungsten rod and parameters of polynomial fits to thermophysical property data (equation (13)). Units of heat capacity C [J kg^{-1} K^{-1}]

Radius a [m]	Length L_0 [m]	Density δ [kg m^{-3}]
1.59766e-3	0.029	19230.0

y	y_0	y_1	y_2	y_3	y_4
C†	−139.83	100.89	11.4817	0.49771	—
α‡	1.3896e-3	−2.4259e-4	3.4818e-4	−3.0597e-5	1.2554e-6
ε†	0.2627	8.1160e-3	—	—	—

†Reference [5].
‡Reference [6].

(1024 pixels). The ambient temperature is 293 K. The maximum temperature for the run, at the midpoint of the rod, was 2880 K.

Fourteen temperature profiles were recorded as the rod cooled over a time period of 1.2168 s. It was found that five profiles could be taken as a set to fit the calculated surface temperatures without falling into the temperature range where there is too much scatter in the data, as discussed in Section 3. Thus, in accordance with the procedure described there, the initial condition for the first set (No. 1) of five profiles is $T^{\exp}(z, t_0)$, the computed profile $T(r, z, t_3)$ at the time corresponding to the fourth profile is the initial condition for the next set (No. 2) of five profiles, $T(r, z, t_6)$ is the initial condition for the third set (No. 3), and $T(r, z, t_9)$ is that for the last set (No. 4). To complete these initial conditions, as can be seen from the end points marked on Fig. 1, extra points are added at the high temperature end of the section when points are removed at the low temperature end. These extra points are taken from the smoothed surface temperature profiles $T^{\exp}(z, t)$ with $t = t_3$, t_6 and t_9, respectively, and with a constant radial temperature gradient δT_N assumed for the interior points, as for the initial condition at $t = t_0$. The coefficients for the boundary conditions (equations (3) and (4) for the time dependence and equations (5) and (6) for the radial dependence) for each set of profiles are listed in Table 2.

Figure 3(a) shows $\Delta(z, t)$ plotted against $T(a, z, t)$ at $t = 0.2808$ s, 0.3744 s, 0.4680 s, 0.5616 s and 0.6552 s, for set No. 2. The criterion that has been used for a good fit is that $\Delta(z, T)$ should be $O(10^{-3})$ over the chosen length of rod and over the chosen time period. This value is within the noise level of the data; about 5 K. To give some idea of the sensitivity of the fit, $\Delta(z, t)$, calculated with the literature values of thermal conductivity [8] for the same set of profiles, No. 2, is shown in Fig. 3(b): at the peak, a six-fold increase in Δ is produced by an 8% decrease in κ. Note that positive values of ΔT correspond to the value of κ being too low.

Once the best fit has been achieved, it is more informative to consider the temperature difference itself,

$$\Delta T(z, t) = T(a, z, t) - T^{\exp}(z, t) \qquad (15)$$

and this is what is shown in Fig. 4 at intervals of 0.0936 s for sets Nos 1, 2, 3 and 4. Here, for ease of discussion, z is expressed in terms of the pixel number. The peak in ΔT at $z = 400$ for the final (lowest temperature) profile of the run (Fig. 4(d)) is probably an artifact of the smoothing process which puts knots at $z = 380$ and 422 for this profile. The four sets of parameters $(\kappa_0, \kappa_1, \kappa_2)$ for the run are listed in Table 3. κ_2 is zero in all cases since the linear case already meets the criterion for a good fit. The parameters

Table 2. (a) Coefficients for boundary conditions at ends of selected sections. See equations (3) and (4): temperatures are scaled in units of $T_0 = 293$ K

No.	$T^{\exp}(a, z_1, t)$	γ_{11} [s^{-1}]	γ_{12} [s^{-2}]	$T^{\exp}(a, z_N, t)$	γ_{21} [s^{-1}]	γ_{22} [s^{-2}]
1	9.2084	−4.7223	0.9312	9.8191	−1.3506	0.2539
2	8.5084	−3.7309	1.4284	9.4662	−1.1875	0.1365
3	8.1720	−2.7359	0.8038	9.1532	−1.0877	0.1322
4	7.8995	−2.1185	0.4348	8.8674	−0.9501	−0.0062

(b) Coefficients for radial gradients at ends of selected sections. See equations (5) and (6)

No.	δT_1 [K]	δT_N [K]
1	9.96	11.72
2	9.96	13.19
3	8.79	13.19
4	7.33	11.72

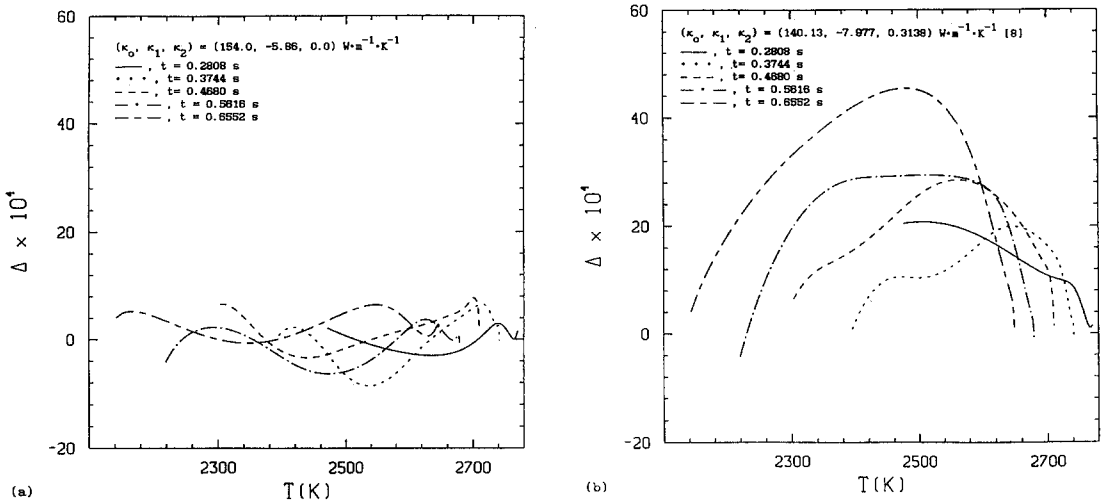

Fig. 3. Fractional difference between calculated and experimental profiles as a function of temperature: $\Delta(z, t)$ vs $T(a, z, t)$. Set No. 2: $t = 0.2808 - 0.6552$ s. (a) Fitted values of κ, (b) literature values of κ [8].

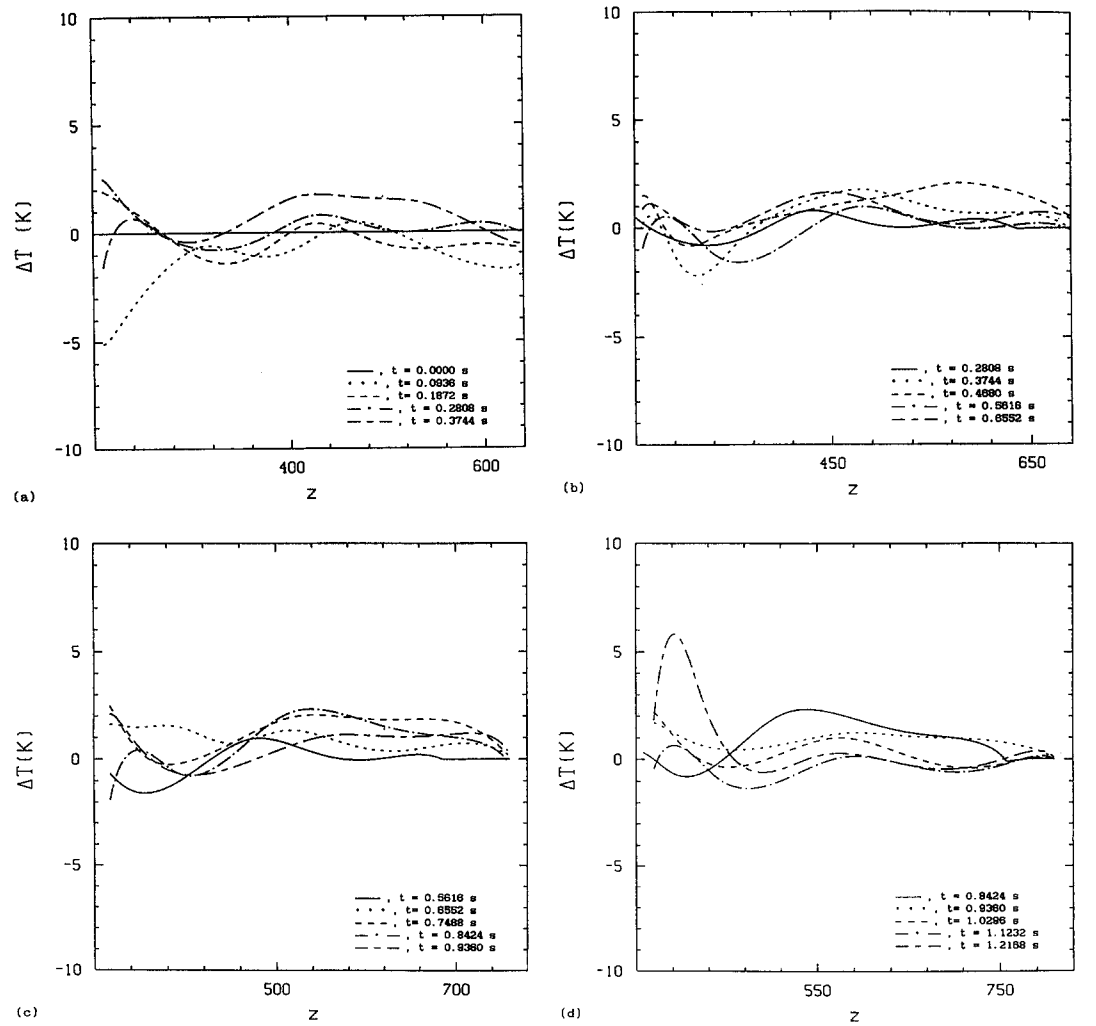

Fig. 4. Difference between calculated and experimental profiles as a function of distance along the rod: $\Delta T(z, t)$ vs z. (a) Set No. 1; (b) set No. 2; (c) set No. 3; (d) set No. 4. The distance along the rod z is measured in units of the pixel size, $p = 2.8325\text{e-}5$ m.

Table 3. Thermal conductivity coefficients κ_i for tungsten rod [W m^{-1} K^{-1}]

No.	κ_0	κ_1	κ_2
1	157.75	−6.590	—
2	154.00	−5.860	—
3	148.25	−5.123	—
4	148.25	−5.123	—
Ref. [8]	140.13	−7.977	0.314

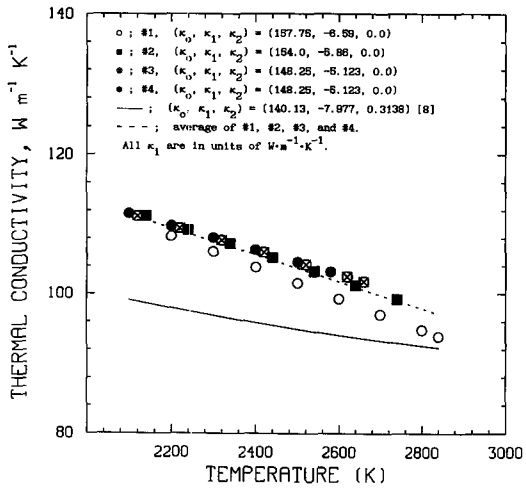

Fig. 5. Thermal conductivity κ vs T(K).

obtained from the thermal conductivity values recommended in the literature [8] are given in Table 3 also.

Finally, the thermal conductivity given by all sets of parameters, including the literature values, is shown in Fig. 5. The literature values lie considerably below the calculated values for temperatures below 2700 K, as one would expect from comparing Δ in Figs. 3(a) and (b). Also shown in Fig. 5, as a guide to the eye, are the average values of κ for the four sets. The greatest deviation of κ from the average value is at the highest temperatures and it is about 3% for set No. 1 and less than 1.5% for the other sets. This is within the estimated accuracy of the input data (heat capacity: 2–3%; thermal expansion: 1–2%; emissivity: 3%; [5, 6]). The deviation of this average from the literature values (estimated accuracy ~5% [8]) goes from 5% to 11% as the temperature falls. Tests with several values of δT_N show that the first set of the run (denoted by open circles) is out of line with the average, mainly because of the initial condition at $t = t_0$ which imposes a constant temperature gradient on the interior points of the rod when only the surface temperature is known. At later times, the calculations show that δT_i varies by several degrees [K] from one end of the rod to the other (see Table 2(b)).

5. CONCLUSIONS

The surface temperature profile is quite sensitive to the values used to represent the thermal conductivity in the region where there is a significant curvature in the profile, as one would expect from the heat transfer equation (equation (2)). As shown by the best fit values in Fig. 4, the difference between the calculated and experimental profiles ΔT can be reduced to a few degrees (better than 0.3%) in all cases; within the scatter of the temperature profile data. Although $\kappa(T)$ itself is consistent over all four sets of profiles to better than 3%, it is of some concern that the results are not in better agreement with the recommended literature values [8]. One factor that may be important is the emissivity of the rod, since radiation is a major cause of heat loss at these high temperatures and emissivity is very dependent on the condition of the emitting surface. The ideal situation would be to measure the emissivity simultaneously. As can be seen from equation (7), the combination ε/κ controls the radiative boundary condition and dominates the heat loss in the horizontal portion of the temperature profile near the center of the rod. If the value of ε is too large, the value needed for κ will also be too large and vice versa. Unfortunately, with the literature values of κ, the $\varepsilon(T)$ that would reduce the large positive value of Δ shown in Fig. 4(b) to an acceptable level, would have to be increased so much at the lower temperatures that it would have a negative slope; an unacceptable result. The discrepancy is therefore unresolved.

It is also possible that the preliminary nature of the experimental data from a newly-developed instrument might contribute to the differences between the κ's calculated from the four sets of profiles and the literature values.

As a result of this investigation of the cooling of a tungsten rod, it appears that the method developed here to determine the thermal conductivity from a comparison between calculated and experimental temperature profiles has some promise. In spite of the relatively small role played by thermal conduction in the heat transfer process compared with thermal radiation, the surface temperature is sensitive to the value of κ, down to the noise level of the data. The question of accuracy posed in the introduction cannot be answered yet, owing to the preliminary nature of the experimental data and to uncertainty about the emissivity of the actual specimen, a particularly important factor in the heat transfer process at these high temperatures. It is to be hoped that this uncertainty will be removed in future experiments.

Acknowledgements—This work was supported in part by the Microgravity Science and Applications Division of NASA. I wish to thank Ared Cezairliyan and Archie Miiller for providing me with their preliminary data so that I could test this method of analysis. I greatly appreciate the help provided by Marjorie McClain in tailoring her program SMOOTH to suit my needs. I also wish to thank Ronald Boisvert for his guidance in the use of PDETWO.

REFERENCES

1. A. Cezairliyan, R. F. Chang, G. M. Foley and A. P. Miiller, High-speed spatial scanning pyrometer, *Rev. Scient. Instrum.* **64,** 1584–1592 (1993).
2. A. Cezairliyan and A. P. Miiller (private communication).
3. H. M. James, Interpretation of direct-heating measurements on a long, but not thin, rod, *High Temp.-High Press.* **11,** 669–681 (1979).
4. D. K. Melgaard and R. F. Sincovec, Algorithm 565, PDETWO/PSETM/GEARB: solution of systems of two-dimensional nonlinear partial differential equations [D3], *ACM Trans. Math. Softw.* **7,** 126–135 (1981).
5. A. Cezairliyan and J. L. McClure, High-speed (subsecond) measurements of heat capacity, electrical resistivity and thermal radiation properties of tungsten in the range 2000–3600 K, *J. Res. Natl. Bur. Stand.* **75A,** 283–290 (1971).
6. A. P. Miiller and A. Cezairliyan, Thermal expansion of tungsten in the range 1500–3600 K by a transient interferometric technique, *Int. J. Thermophys.* **11,** 619–628 (1990).
7. M. McClain, private communication.
8. Y. S. Touloukian, R. W. Powell, C. Y. Ho and P. G. Klemens, Recommended thermal conductivity of tungsten. In *Thermal Conductivity, Metallic Elements and Alloys,* Vol. 1 of *TPRC Series on Thermophysical Properties of Matter* (Edited by Y. S. Touloukian and C. Y. Ho), p. 428. Plenum, New York (1970).